

# ASSESSMENT OF MULTISCALE MODELS FOR LES: SPECTRAL BEHAVIOUR IN VERY HIGH REYNOLDS NUMBER TURBULENCE AND CASES WITH AIRCRAFT WAKE VORTICES.

**Laurent Bricteux, Roger Cocle, Matthieu Duponcheel, Laurent Georges\*, Grégoire Winckelmans**

Mechanical Engineering Department, Division TERM,  
also Center for Systems Engineering and Applied Mechanics (CESAME)  
Université catholique de Louvain (UCL)  
Louvain-la-Neuve, Belgium

\*Center for Research in Aeronautics (CENAERO),  
Gosselies, Belgium

corresponding author: bricteux@term.ucl.ac.be

## ABSTRACT

The aim of this study is to compare several subgrid scale (SGS) models in terms of their ability to correctly dissipate energy for LES at high Reynolds number, with a good spectral behavior. We consider first homogeneous isotropic turbulence (HIT), then more complex flows involving large vortical structures: aircraft wake vortices interacting with turbulence, and aircraft wake vortices interacting with a ground. The performance of the SGS models used is assessed for each of these flows.

## INTRODUCTION

Performing LES of turbulent flows requires quality SGS models with a good spectral behavior. They should also dissipate energy only when and where it is required. The numerical codes used to perform such simulations should also be of high quality: energy conserving discretization schemes and accurate time stepping.

## NUMERICAL METHODS

The governing equations are the classical Navier-Stokes equations for incompressible flows with constant viscosity and supplemented by a subgrid scale model.

$$\nabla \cdot \mathbf{u} = 0 \quad (1)$$

$$\frac{\partial \mathbf{u}}{\partial t} + (\mathbf{u} \cdot \nabla) \mathbf{u} = -\nabla P + \nu \nabla^2 \mathbf{u} + \nabla \cdot \tau^M, \quad (2)$$

where  $P$  is the reduced pressure,  $\nu$  is the kinematic viscosity, and  $\tau^M$  is the SGS stress tensor model. We present hereafter the three methods that we use to solve these equations.

### Pseudo-spectral Navier-Stokes solver

The Navier-Stokes solver considered here is based on the Fourier-Galerkin pseudo-spectral methodology. The time integration of equation (2) is carried out in spectral space using a technique in which the convective and subgrid scale model terms are marched explicitly using the 3rd order Williamson scheme. The nonlinear term is evaluated using a pseudo-spectral algorithm and the dealiasing is done using a phase shift procedure as explained in Canuto et.al. (1988), which ensures energy conservation.

### Vortex-in-cell code

The Navier-Stokes equations are solved in their vorticity-velocity formulation:

$$\frac{D\boldsymbol{\omega}}{Dt} - \nabla \cdot (\mathbf{u}\boldsymbol{\omega}) = \nu \nabla^2 \boldsymbol{\omega} + \nabla \cdot \mathbf{T}^M \quad (3)$$

with  $\boldsymbol{\omega} = \nabla \times \mathbf{u}$  the vorticity field and  $\mathbf{T}^M$  the SGS model. The numerical solution of (3) is obtained following the vortex-in-cell (VIC) approach. The vorticity field is represented by regularized vortex particles:

$$\boldsymbol{\omega}_\sigma(\mathbf{x}, t) = \sum_p \alpha_p(t) \frac{1}{(\sqrt{\pi}\sigma)^3} \exp\left(-\frac{|\mathbf{x} - \mathbf{x}_p(t)|^2}{\sigma^2}\right), \quad (4)$$

with  $\alpha_p = \int \boldsymbol{\omega} d\mathbf{x} = \boldsymbol{\omega}_p h^3$  the strength of particle  $p$ ,  $\mathbf{x}_p$  its position,  $h$  the discretization size (grid size, also used for particle redistribution), and  $\sigma$  the regularization parameter. Interpolations between particles and grid, as well as particle redistribution, are all done using the  $M'_4$  scheme. The vector streamfunction  $\boldsymbol{\psi}$  is obtained by solving the Poisson equation  $\nabla^2 \boldsymbol{\psi} = -\boldsymbol{\omega}$  on the grid, using 4th order finite differences (FD). The velocity field (needed for convection and stretching) is then obtained from  $\mathbf{u} = \nabla \times \boldsymbol{\psi}$ , also using FD. The convective part (i.e., the lhs of (3) is done using the Lagrangian approach:  $d\mathbf{x}_p/dt = \mathbf{u}(\mathbf{x}_p)$ ; this ensures good convection (i.e., negligible dissipation and dispersion errors). The time variation of the particle strengths (i.e., the rhs of (3) including both the vorticity stretching and the dissipation terms) is evaluated on the grid, using FD. The global time marching procedure is carried out using the Leap Frog scheme for the convection and the Adams-Bashforth scheme for the diffusion. Finally, the divergence-free character of the vorticity field is maintained by a proper re-projection of the discrete vorticity field, which also requires solving a Poisson equation. The details of the method are presented in (Cocle et al., 2007).

### Fourth order finite differences code

The equations (1) and (2) are solved using a fractional-step method with the ‘‘delta’’ form for the pressure described by Lee et al. (2001). The convective term is integrated using an Adams-Bashforth 2 scheme and the diffusion term using an implicit Crank-Nicolson scheme. The equations are discretized in space using the fourth order finite difference

scheme of Vasilyev (2000). This discretization of the convective term conserves energy on Cartesian stretched meshes. The Poisson equation for the pressure is solved using an efficient multigrid solver with a line Gauss-Seidel smoother.

## SUBGRID SCALE MODELING

First, we classify the multiscale subgrid scale models in two sets, according to the spectral content of the field on which they are acting:

- *Type I* models: models acting on the complete LES field. The SGS stress is then modelled using  $\tau_{ij}^M = 2\nu_{\text{sgs}} S_{ij}$  with  $S_{ij} = \frac{1}{2} \left( \frac{\partial u_i}{\partial x_j} + \frac{\partial u_j}{\partial x_i} \right)$  the strain rate tensor. For the vorticity formulation, we use  $T_{ij}^M = 2\nu_{\text{sgs}} Q_{ij}$  with  $Q_{ij} = \frac{1}{2} \left( \frac{\partial \omega_i}{\partial x_j} + \frac{\partial \omega_j}{\partial x_i} \right)$ .
- *Type II* models: models acting on a “small-scale” LES field. The SGS stress is then modelled using  $\tau_{ij} = 2\nu_{\text{sgs}} S_{ij}^s$  with  $S_{ij}^s$  the strain rate tensor of the small scale field. For the vorticity formulation, we use  $Q_{ij}^s$ .

The small-scale field is obtained in the finite difference code and in the VIC code by using the compact (stencil 3) tensor-product discrete filter, and that is iterated  $n$  times to produce an order  $2n$  filter (Jeanmart and Winckelmans, 2002, 2007):  $\mathbf{u}^{s(n)} = \mathbf{u} - \bar{\mathbf{u}}^{(n)}$  with

$$\bar{\mathbf{u}}^{(n)} = \left( I - \left( -\delta_x^2/4 \right)^n \right) \left( I - \left( -\delta_y^2/4 \right)^n \right) \left( I - \left( -\delta_z^2/4 \right)^n \right) \mathbf{u}$$

where  $\delta_x^2 f_{i,j,k} = f_{i+1,j,k} - 2f_{i,j,k} + f_{i-1,j,k}$ . In Fourier space, the filtered field is:

$$\widehat{\bar{\mathbf{u}}^{(n)}}(\mathbf{k}) = \begin{pmatrix} \left( 1 - \sin^{2n} \left( \frac{k_x h_x}{2} \right) \right) \\ \left( 1 - \sin^{2n} \left( \frac{k_y h_y}{2} \right) \right) \\ \left( 1 - \sin^{2n} \left( \frac{k_z h_z}{2} \right) \right) \end{pmatrix} \widehat{\mathbf{u}}(\mathbf{k}) \quad (5)$$

This classification can be further extended according to the field on which  $\nu_{\text{sgs}}$  is evaluated (complete or small). The length scale is here defined as:  $\Delta = (h_x h_y h_z)^{1/3}$ . All the constants used for the different models were carefully calibrated on HIT flows.

### Type I models

We first present the “x-complete” models. The classical Smagorinsky (SMAG) model is the most common “complete-complete” model:

$$\nu_{\text{sgs}} = C_S \Delta^2 (2 S_{ij} S_{ij})^{1/2}.$$

The value of the model coefficient is  $C_S = 0.027$ . A second model is the FSF model (Ducros et al., 1996) (a “small-complete” model). Here, the subgrid viscosity is obtained from the “filtered structure function”  $F_2^{s(n)}$ :

$$\nu_{\text{sgs}} = C_F^{(n)} \Delta \sqrt{F_2^{s(n)}},$$

where

$$F_2^{s(n)} = \left\langle \left\| \mathbf{u}^{s(n)}(\mathbf{x} + \mathbf{x}') - \mathbf{u}^{s(n)}(\mathbf{x}) \right\|^2 \right\rangle_{|\mathbf{x}'| = \Delta}. \quad (6)$$

The model coefficient value is  $C_F^{(1)} = 0.078$ . This structure function is evaluated using the nearest neighbors ( $3^3 = 27$ ) values. The small-scale field  $\mathbf{u}^{s(n)}$  is here obtained by recursive application ( $n$  times) of the 2nd order FD Laplacian:

$$\mathbf{u}^{s(n)} = \left( -\frac{\Delta^2}{4} \nabla^2 \right)^n \mathbf{u}.$$

The model has also been shown to capture well the transition to turbulent flow that results from the growth of instabilities in wake vortex simulations (Cocle et al., 2006). A third model is the SMAG2 model (a “small-complete” model):

$$\nu_{\text{sgs}} = C_{S_2}^{(n)} \Delta^2 (2 S_{ij}^s S_{ij}^s)^{1/2}.$$

The coefficient value with  $n = 1$  is  $C_{S_2}^{(1)} = 0.045$ .

### Type II models

We now present the “x-small” models, thus those where the SGS viscosity is applied on the small-scale field ( $\mathbf{u}^s$  or  $\boldsymbol{\omega}^s$  depending on the formulation for the Navier-Stokes equations). The first “complete-small” model is the “regularized” version, here using the tensor product discrete filter, of the “variational multiscale” model (VM) of Hughes et al. (2001), see (Jeanmart and Winckelmans, 2002). The RVM model was also further proposed and tested by Vreman et al. (2003) and also by Stolz et al. (2004, 2005). In the present work, we use

$$\nu_{\text{sgs}} = C_R^{(n)} \Delta^2 (2 S_{ij} S_{ij})^{1/2},$$

with  $C_R^{(1)} = 0.036$  and  $C_R^{(3)} = 0.060$ . The second model considered is the regularized version of the “small-small” variational multiscale model. We use

$$\nu_{\text{sgs}} = C_{R_2}^{(n)} \Delta^2 (2 S_{ij}^s S_{ij}^s)^{1/2},$$

which is here noted RVM2. This model was proposed and evaluated by Vreman et al. (2003) and by Stolz et al. (2004, 2005). The coefficient values are  $C_{R_2}^{(1)} = 0.066$  and  $C_{R_2}^{(3)} = 0.011$ .

### High order hyperviscosity model

The hyperviscosity (HV) formulation used in this study provides a SGS dissipation term acting solely at the very small scales of the LES grid (e.g. compared to RVM and RVM2). Previous studies (Cocle et al., 2006) of four vortex system flows showed that this model performs well for turbulent wake vortex simulations. The SGS model is taken as

$$\tau_{ij}^M = (-1)^p 2 \nu_h \nabla^{2p} S_{ij}.$$

On a uniform grid and using a global time scale  $T_0$  in the SGS model (for simplification), this leads to:

$$\nabla \cdot \hat{\tau}^M(\mathbf{k}) = -C^{(p)} (kh)^{2(p+1)} \frac{1}{T_0} \widehat{\mathbf{u}}(\mathbf{k}).$$

In the present study, we used  $p = 7$ .

## HOMOGENEOUS TURBULENCE FLOW

We are interested in LES of decaying HIT in the limit of very high Reynolds number (i.e. simulations where the molecular viscosity dissipation is negligible compared to the SGS dissipation). Thus, we here deliberately run LES with  $\nu$  set to zero. The results presented were using the VIC

and the pseudo-spectral codes. The initial condition was build following the algorithm described by Rogallo (1981). This initial field then evolved using LES. For the investigations using the VIC code, the following SGS models are used: SMAG, FSF (with  $n = 1$ ) and RVM (with  $n = 1$  and  $n = 3$ ); RVM2 and FSF2. Simulations were also carried out using the pseudo-spectral code. The models investigated are in this case the SMAG model, the RVM2 (with  $n = 3$ ) model and the high order hyper-viscosity (HV) model. Fig. 1 shows the obtained energy spectra for  $128^3$  grid (also time-averaged between  $t = 10$  and  $40$ , i.e. when the turbulence is statistically converged). We observe that the *Type II* models with  $n = 3$  provide the broader inertial range (i.e., with  $k^{-5/3}$  behavior). The width of this captured inertial range decreases with the order of the filter used to compute the small-scale field (compare RVM with  $n = 1$  to RVM with  $n = 3$ ). In opposition, the FSF and the SMAG models do not exhibit any inertial range on such  $128^3$  grid. Nevertheless, all spectra are clearly altered by a “bump-like” behavior at the medium wavenumbers, though to a lesser extent, for the *Type II* models using high order ( $n = 3$ ) filters. This non-physical energy accumulation is present because the shape of the dissipation spectra of the SGS models is never exactly the required one. However, the behavior is improved when the *Type II* models are used (especially with high order filters); yet it does not prevent this “bottleneck” effect in the energy cascade. As they act only at the small scales (comparing to the *Type I* models), their influence on the large scales is reduced and allows, to capture a true  $k^{-5/3}$  inertial range. This conclusion is also valid for the spectrum obtained using the HV dissipation model: it provides an inertial range as broad as the *Type II* models with  $n = 3$ , yet the energy “bump” is more pronounced. This result compares well with Lamorgese et al. (2005) who shows the presence of the “bottleneck” effect in the energy spectra when a hyper-viscous dissipation is used. We also investigate the asymptotic behavior of the models when performing LES on larger grids, see Fig. 2. We consider the SMAG model, the RVM2 model and the HV model, and we compare the shape of the spectra obtained using the spectral code and higher resolution. We also show the unequivocal presence of the “bump-like” behavior. As expected, the  $k^{-5/3}$  inertial range becomes broader as the grid is taken larger. Such LES has indeed reached its “asymptotic behavior”, with self-similar obtained spectra.

## AIRCRAFT WAKE VORTICES IN LOW LEVEL TURBULENCE

The fluid flow considered here is related to the passage of a heavy aircraft in a turbulent atmosphere. This is adequately simulated by the superposition of an homogeneous isotropic turbulent flow (obtained as a pre-simulation, letting a turbulent field decay down to a prescribed level of dissipation) and a pair of analytical counter rotating vortices. The LES models investigated are the RVM2 model and HV. These simulations are performed using the pseudo-spectral code.

### Description of the flow

Once the homogeneous isotropic turbulent flow is obtained, it is required to choose a distribution function to initialize the wake flow. In the present work, a low order algebraic velocity profile was used:

$$u_\theta(r) = \frac{\Gamma_0}{2\pi r} \frac{r^2}{(r^2 + r_c^2)}.$$

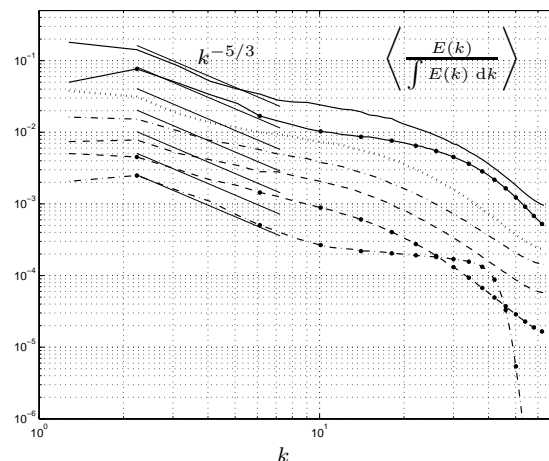


Figure 1:  $128^3$  LES at very high Reynolds number: normalized energy spectra (also time-averaged between  $t = 10$  and  $40$ ; the curves are shifted vertically by 0.5 to better distinguish them): 1) using the VIC method: SMAG (*dash*), FSF (*dash-dot*), RVM with  $n = 1$  (*dot*) and with  $n = 3$  (*solid*); 2) using the pseudo-spectral method: SMAG (*dash with bullets*),  $(kh)^{16}$  HV (*dash-dot with bullets*) and RVM2 with  $n = 3$  (*solid with bullets*).

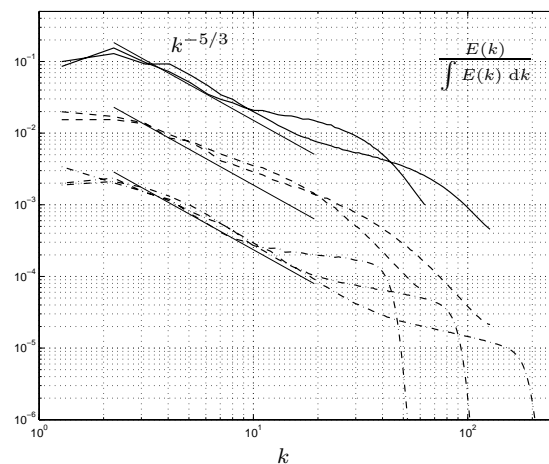


Figure 2: LES at very high Reynolds number: Asymptotic behavior of the obtained energy spectra when using larger grids (pseudo-spectral method at  $t = 20$ ; the curves are shifted vertically by 0.125 to better distinguish them): RVM2 with  $n = 3$  on  $128^3$  and  $256^3$  grids (*solid*), SMAG on  $128^3$  and  $256^3$  grids (*dash*),  $(kh)^{16}$  HV on  $128^3$ ,  $256^3$  and  $512^3$  grids (*dash-dot*).

The parameter  $r_c$  is the radius of maximum tangential velocity and was here set to  $r_c = 0.05 b_0$ , which is a realistic value for aircraft wake vortices after roll-up. The vortex cores are well discretized ( $h/b_0 = 1/64$ ). The dimensional parameters of this flow are given in Table 1. The computational domain is periodic in the three directions and the periodicity lengths are chosen to ensure that the periodic images only have a minor influence on the wake vortex pair. As the obtention of a vortex system in a turbulent state is the aim of this investigation, we do not allow for the long wavelength Crow instability to develop. This explains the limited extension of the domain along the vortex direction. The initial descent velocity of this pair of vortices is:  $V_0 = \frac{\Gamma_0}{2\pi b_0}$ . This

Table 1: Physical parameters of the wake vortex flow

Vortex circulation	$\Gamma_0$	$400 \text{ m}^2/\text{s}$
Vortex spacing	$b_0$	$50 \text{ m}$
Dissipation level	$\epsilon$	$10^{-5} \text{ m}^2/\text{s}^3$
Periodicity length	$L_x, L_y, L_z$	$4 b_0$
Number of Fourier modes	$N_x, N_y, N_z$	256

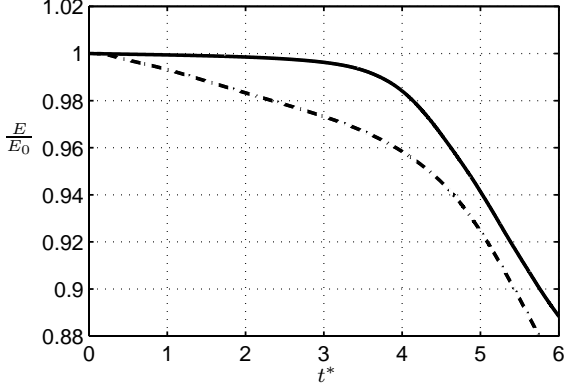


Figure 3: Evolution of the kinetic energy for the aircraft wake two vortex system.  $(kh)^{16}$  HV (solid) RVM2 model with  $n = 3$  (dash-dot).

velocity is used as velocity scale. The dimensionless time is  $t^* = t \frac{V_0}{b_0}$ . In the same way,  $E^* = \frac{E}{V_0^2}$  and  $\epsilon^* = \frac{\epsilon b_0^3}{V_0^3}$ . Taking the value of air viscosity, we find an order of magnitude for the Reynolds number of this flow as  $Re = \frac{U_0}{\nu} \approx 3 \times 10^7$ . The dissipation due to the molecular viscosity thus plays a very minor role compared the subgrid scale model dissipation. For this reason, we deliberately set  $\nu$  to zero.

## Results

A visualization of the flow is provided in Fig.7. The vortex system engulfs the ambient turbulence, the non-linear interactions then amplify it and this eventually leads to a vortex pair where the surrounding turbulence is independent of the atmospheric background: the low level turbulence thus acts as a seed to create a “turbulent vortex pair” that then lives and decays on its own. The kinetic energy evolution of the flow is provided in Fig.3. The curves exhibit a similar global behavior: a first period where the global kinetic energy is essentially conserved, followed by a decay phase when the turbulence is established. One can remark that the energy curve when using the RVM2 model decays sooner than when using the HV model. This is due to the fact that the RVM2 model is acting as soon as the stretching of the turbulent structures by the strong vortices creates medium scales. Both SGS models eventually leads to a turbulent flow with similar dissipation see Fig.4.

## AIRCRAFT WAKE VORTICES IN GROUND EFFECT

Another challenging wake vortex case, of great practical interest, is the interaction of an aircraft two-vortex system with the ground. The simulation of this flow requires a subgrid-scale model that is able to handle both vortical and wall-bounded flows, as well as transitional flows. We have performed wall-resolved LES of this flow, at moderate Reynolds number, and using two different subgrid-scale models.

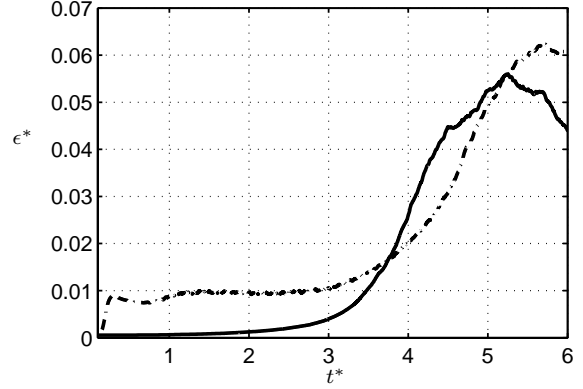


Figure 4: Evolution of the normalized dissipation  $\epsilon^* = \epsilon b_0 / V_0^3$  for the aircraft wake two vortex system.  $(kh)^{16}$  HV (solid) RVM2 model with  $n = 3$  (dash-dot).

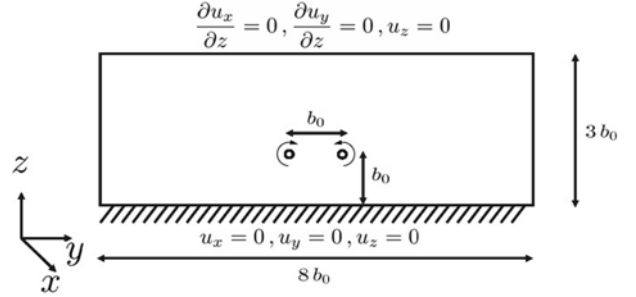


Figure 5: Sketch of the computational domain. The domain is extruded in the  $x$  direction.

### Description of the flow

The flow consists in a pair of counter rotating vortices interacting with the ground. This simulates quite realistically the wake vortex system in the far field of an aircraft flying close to the ground (after completion of the initial roll-up). This flow was simulated using the fourth order finite difference code. Defining the initial distance between the vortex centers as  $b_0$ , the lengths of the computational domain are  $L_x = 4 b_0$ ,  $L_y = 8 b_0$  and  $L_z = 3 b_0$ . The definitions of the descent velocity  $V_0$  and the dimensionless time  $t^*$  are the same as in the previous flow. The Reynolds number  $Re = \Gamma_0 / \nu$  is here set to 20000. Considering boundary conditions, the domain is periodic in the  $x$  and  $y$  directions. A no-slip condition is set at the ground ( $z = 0$ ) and a slip condition at the top of the computational domain ( $z = 3 b_0$ ). The number of grid points is  $(N_x \times N_y \times N_z = 256 \times 512 \times 256)$ . The grid is refined in the wall-normal direction to properly capture the boundary layers. The vortices are also modeled using low order algebraic velocity profiles with  $r_c = 0.05 b_0$ . The first subgrid model investigated is the Smagorinsky model scaled using the Piomelli damping to obtain  $\nu_{sgs} \propto y^3$  near the wall:

$$\nu_{sgs} = F_p C_S \Delta^2 (2 S_{ij} S_{ij})^{1/2},$$

where  $C_S = 0.027$  and  $F_p = 1 - \exp(-(y^+ / 25)^3)$ . this is thus a “complete-complete” model. The second model investigated is a “small-complete” one for which the effective viscosity is also damped near the ground:  $\nu_{sgs} = F_p C_{S2}^{(3)} \Delta^2 (2 S_{ij}^s S_{ij}^s)^{1/2}$ , with  $n = 3$  and  $C_{S2}^{(3)} = 0.063$ .

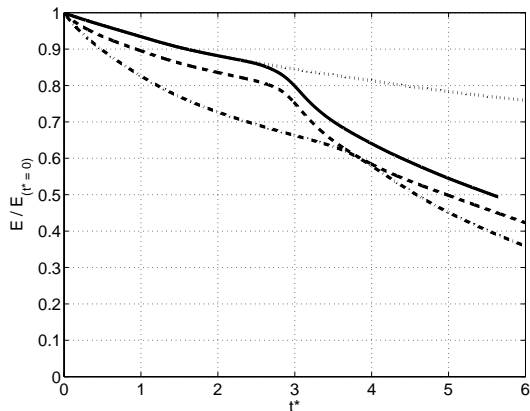


Figure 6: Evolution of the energy: LES at  $Re = 200000$  using the small-complete model (*solid*) and using the Smagorinsky model (*dash*); the DNS at  $Re = 5000$  (*dash dot*); the 2-D DNS at  $Re = 200000$  (*dot*).

### Results

We provide a visualization of this flow at Fig. 8. At time  $t^* = 0$ , the vortices create very thin boundary layers at the ground. The vortices move down due to their mutual induced velocity. Each boundary layer separates, leading to the formation of secondary vortices which orbit around the main vortex cores. The secondary vortices are unstable with respect to short-wave (elliptic) instabilities. Their non-linear interaction with the primary vortices eventually results in a turbulent vortex system with much enhanced decay rate. The kinetic energy evolution of the flow is also provided in Fig.6. Comparing the energy curves with the 2D DNS of reference, we observe that the vortex dynamics in the initial laminar phase is well captured with the small-complete model while it is not with the classical Smagorinsky which dissipates too much. The small complete model is well adapted for LES of such transitional flow as it does not dissipates in the well resolved and/or laminar regions.

### CONCLUSIONS

In the first part of this study, the results obtained by performing LES of HIT flow allowed us to highlight the good spectral behaviour of subgrid models acting on a small field. Considering this, we chosen the RVM2 model to perform LES of aircraft wake vortex system interacting with turbulence at very high Reynolds number. The comparison with the HV model showed that the RVM2 models attains a dissipation level which is of the same order of magnitude have a good better spectral behaviour. Then LES of aircraft wake vortex system in ground effect was performed and allowed us to conclude that the small complete model is well suited to simulate transitional flows in presence of walls and vortical structures. We showed thus that the multiscale subgrid models acting on small fields performs fairly well on several complex flows. Moreover, one of the original aspect of this work is that all the LES simulations were performed on large grids at very large Reynolds number.

### ACKNOWLEDGMENTS

The simulations were done using the facilities of the Calcul Intensif et Stockage de Masse (CISM) on the Lemaitre cluster funded by Fond National de Recherche Scientifique (FNRS) under a FRFC Project and by UCL (Fonds Spéciaux de Recherche). Part of he results were obtained in the

framework of the “LASEF” project funded by the “Région Wallonne” of Belgium and the “FARWAKE” project funded by the European Commission. M.Duponcheel is a FNRS research fellow.

### REFERENCES

- Cocle R., Dufresne L. and Winckelmans G., Investigation of multiscale subgrid models for LES of instabilities and turbulence in wake vortex systems, *Complex Effects in LES: Springer volume*, LNCSE series, 2006.
- Cocle R., Winckelmans G., Daeninck G. and Thirifay F., An efficient combination of vortex-in-cell and fast multipole methods, submitted to *J. Comp. Phys.*, April (2007).
- Ducros F., Comte P. and Lesieur M., Large-eddy simulation of transition to turbulence in a boundary layer spatially developing over a flat plate, *J. Fluid Mech.*, **326**, 1–36 (1996).
- Hughes T.J.R., Mazzei L., Oberai A.A. and Wray A.A., The multiscale formulation of large eddy simulation: decay of homogeneous isotropic turbulence, *Phys. Fluids*, **13**, 505–512 (2001).
- Jeanmart H. and Winckelmans G., Comparison of recent dynamic subgrid-scale models in turbulent channel flow, *Proc. Summer Program 2002*, Center for Turbulence Research, Stanford University and NASA Ames, 105–116 (2002).
- Jeanmart H. and Winckelmans G., Investigations of eddy-viscosity models modified using discrete filters: a simplified “regularized variational multiscale model” and an “enhanced field model”, to appear in *Physics of fluids*, (2007).
- Lamorgese A. G., Caughey D. A., Pope S. B., Direct numerical simulation of homogeneous turbulence with hyper-viscosity, *Phys. Fluids*, **17**, 015106 (2005).
- Lee, M.J. and Oh, B.D. and Kim, Y.B., Canonical Fractional-Step Methods and Consistent Boundary Conditions for the Incompressible Navier Stokes Equations, *J. J.Comp. Phys.*, vol.168, 2001, 73-100.
- Rogallo R., Numerical experiments in homogeneous turbulence, Technical Report No. NASA Tech. Memo. 81315, NASA Ames Research Center (1981).
- Stolz S., Schlatter P., Meyer D. and Kleiser L., High-pass filtered eddy-viscosity models for LES, *Direct and Large-Eddy Simulation V*, edited by Friedrich R., Geurts B.J. and Métails O., Kluwer, 81–88 (2004).
- Stolz S., Schlatter P. and Kleiser L., High-pass filtered eddy-viscosity models for large-eddy simulations of transitional flow, *Phys. Fluids*, **17**, 065103 (2005).
- O.V. Vasilyev, High order finite difference schemes on non-uniform meshes with good conservation properties, *J. Comp. Phys.*, vol. 157(2), pp 746-761, 2000.
- Vreman A.W., The filtering analog of the variational multiscale method in large-eddy simulation, *Phys. Fluids*, **15**, L61 (2003).

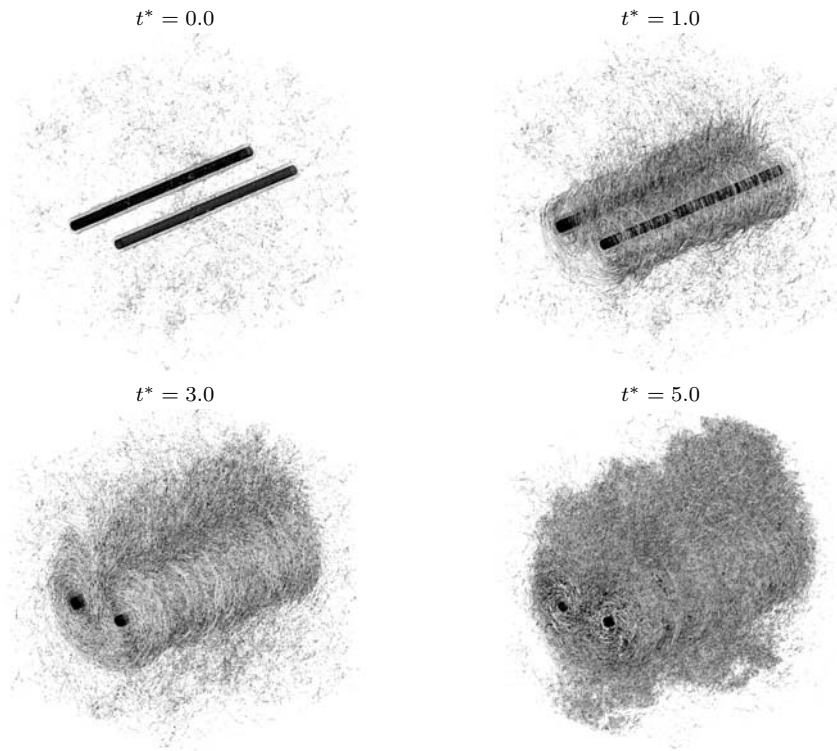


Figure 7: Aircraft wake two vortex system interacting with low level turbulence: iso vorticity surfaces at different times and for two levels of  $\|\omega\| b_0^2/\Gamma_0 = 2$  (low opacity) and 10 (high opacity).

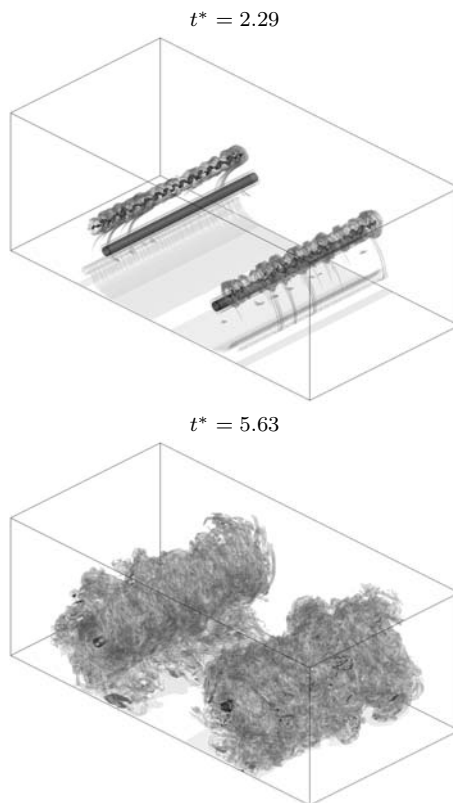


Figure 8: Aircraft wake two vortex system in ground effect: iso vorticity surfaces at different times and for two levels of  $\|\omega\| b_0^2/\Gamma_0 = 2$  (low opacity) and 10 (high opacity).